LIQUID HYDROGEN POOL EVAPORATION ABOVE FOUR DIFFERENT SUBSTRATES

Friedrich, A.[1*], Breitung, W.[2], Veser, A.[2], Kuznetsov, M.[1], Gerstner, J.[2], Jordan, T.[1]

[1] Karlsruhe Institute of Technology, 76344, Eggenstein-Leopoldshafen, Germany
[2] Pro-Science GmbH, 76275, Ettlingen, Germany

***Corresponding author's email address: andreas.friedrich@kit.edu**

ABSTRACT

In the frame of the EC-funded project PRESLHY ten experiments on LH2-pool evaporation above four different substrates have been performed with the POOL-facility on a free field test site. Substrates to be investigated comprised concrete, sand, water and gravel. Four of the experiments were made with artificial side wind of known direction and known velocity to investigate the influence of side wind on hydrogen evaporation and cloud formation above the LH2-pool. The POOL-facility mainly consists of an insulated stainless-steel box with the dimensions 0.5 x 0.5 x 0.2 m³ that is filled up to half the height (0.1 m) with the respective substrate and LH2. The height of the LH2-pool that forms above the substrate can be determined using the weight of the complete facility, which is positioned on a scale. Additionally, six thermocouples are located in different heights above the substrate surface to indicate the LH2-level as soon as they are covered with LH2. Further measurement equipment used in the tests comprises temperature measurements inside the substrate and several thermocouples in the unconfined space above the pool, where also H2-concentration measurements were performed. Using the sensor information, pool evaporation rates for the different substrates were determined. The temperature and concentration measurements above the pool were mainly used to define promising ignition positions for subsequent combustion experiments, in which the LH2-spills above the different substrates were ignited.

1.0 INTRODUCTION

Hydrogen is the first element in the periodic table of the elements and thus hydrogen is the lightest known fuel. With a caloric value of Q = 120 MJ/kg is has a relatively high gravimetric energy density, but due to the low density of gaseous hydrogen (GH2) at ambient conditions (ρ = 0.09 kg/m³) it has a very low volumetric energy density of Q = 10.8 MJ/m³ (compared to e.g. Q = 45 MJ/m³ for methane). To reach competitive operating distances, hydrogen powered vehicles need rather large tanks with thick walls to store the required amount of gaseous hydrogen at elevated pressures (e.g. 700 bar for passenger cars), or might be equipped with much smaller tanks, when the fuel is carried as a liquid (LH2) at a temperature of approx. 20 K (-253 °C). This cryogenic liquid hydrogen is the lightest chemical fuel and compared to compressed GH2 it may be stored at moderate pressure in light weighted cryostats. Therefore, it has been used as a fuel in space missions for decades and because of its CO2 reduction potential, it is currently becoming increasingly attractive in aviation.

In safety considerations on LH2-transport and refueling, leakages or failures may lead to LH2-releases to the environment. These spills will produce large clouds of GH2, and might even from pools, depending on the amount of LH2 and the nature of the ground (or substrate) that is exposed to the LH2. The vaporization of the pool and the mixing of GH2 with air is the first step in an accident scenario leading to the generation of a flammable cloud of H2/air mixture that might produce huge temperature and pressure loads in case of an ignition. So the evaporation rates of LH2 from pools above different substrates are of fundamental interest for safety assessments of LH2 applications, but only limited data on the scenario are available. Most of the data concentrate on free spills above flat grounds and water surfaces, where mostly expansion and shrinking of the puddle is investigated and computational models are proposed [1-7]. Only few data is available for confining basins, in which LH2-pools of considerable depth might form and where the evaporation is governed by the heat transfer from the ground material.

In the current work, the evaporation of LH2-pools with a depth of approx. 10 cm and an area with a square ground face of 0.25 m² above four different substrates that might be found close to LH2 applications is investigated. The substrates investigated are concrete, sand, water and gravel.

2.0 FACILITY DESCRIPTION

The POOL-facility was installed on a remote free-field test site in the forest outside KIT Campus North, where, for several experimental series' in the frame of the EC-funded project PRESLHY, a LH2-trailer was parked. Fig. 1 shows the main parts of the facility and photos of the four boxes with the substrates investigated.

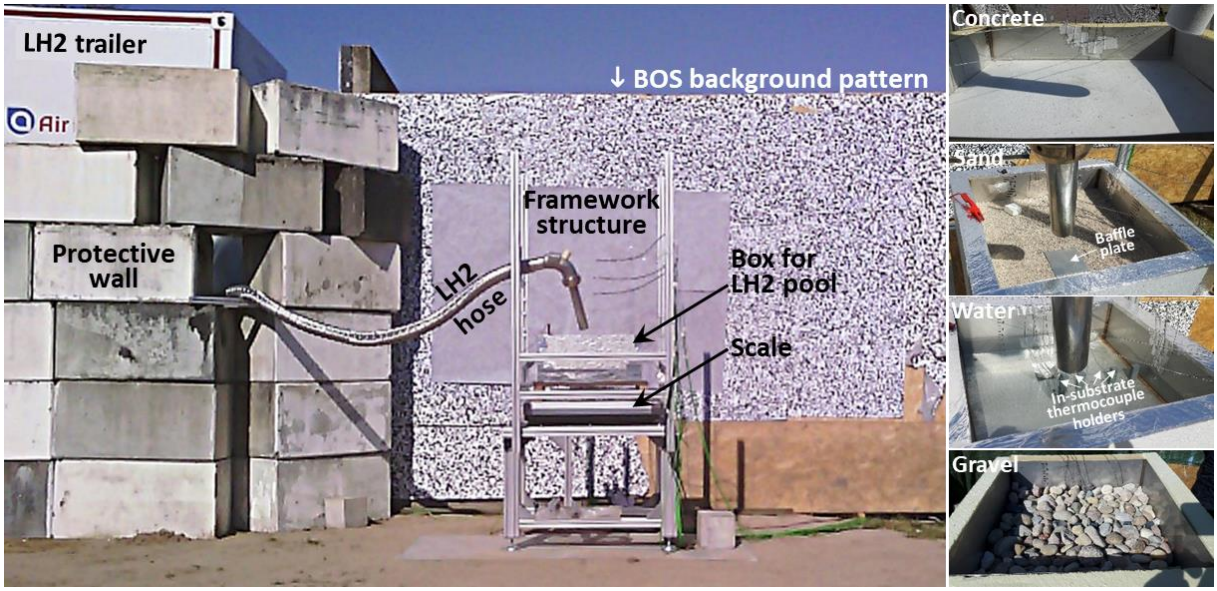

Figure 1. Photo with main parts of the POOL-facility (left) and boxes with the four substrates investigated (right).

Behind the door at the rear end of the LH2-trailer, the control panel with all valves and joint points is located and so this door has to remain opened during any LH2-withdrawal from the trailer. For protection of this vulnerable part of the trailer a protective wall of concrete bricks (M = 500 kg/brick) was constructed between trailer and experiment. This crowded layout of the components was necessary due to the limited length of the super insulated hose (L ≈ 5 m) that was used to generate the LH2-pools in the boxes of the facility (right part of Fig. 1). A substrate-filled box was positioned below the LH2 hose on a scale. The hose was fastened to a surrounding framework structure that has no mechanical contact to the pool and especially the scale. Behind the facility, next to the LH2-trailer a massive container was positioned, in front of which a wall with random pattern for applying the BOS-method to the various optical records that were captured during the experiments, was positioned.

The POOL-facility itself mainly consists of a stainless-steel box (dimensions 0.5 x 0.5 x 0.2 m³) that is filled up to half the height (0.1 m) with different substrates that can be found in, or are feasible for various real LH2-applications. The substrates used in the tests were water, concrete, sand and gravel, with the concrete pool being prepared already more than 1 month prior to the first experiment to allow sufficient hardening and drying. For thermal insulation, the sidewalls and ground plate of the boxes were insulated with Styrofoam plates.

The insulated steel box of the POOL-facility was positioned on a scale (Mettler-Toledo, Type: PBA430x, 0 - 150 kg) to monitor the mass of LH2 accumulated in the pool during the filling and evaporation periods of an experiment. During preparation, special care was taken to eliminate all influences on the signal of the scales that might be caused by wires and hoses that are connected to the

facility. For the evaluation of the records, usually the offset of the scale signal at the beginning of the release was subtracted from the measured values to start the experiment at a weight value of 0 kg.

The filling level of the pool was also monitored by 6 thermocouples that were installed above the substrate surface on the inner steel wall or in the center of the box in different heights (magenta dots in left part of Fig. 2). Further 8 thermocouples were distributed on holders inside the substrate (orange dots), and 12 thermocouples (red dots), together with 3 thin tubes for continuous gas sample extraction (blue squares), were positioned via wires in the framework structure above the box. Through the 3 thin tubes gas samples were transported from the sampling position to 3 H2-sensors that continuously analyzed the samples. The various thermocouple and sample taking positions are sketched in the left part of Fig. 2. The records of sensors with labels are used in this work, while the other records were omitted in the graphs for clarity, or are incidental to the present investigation.

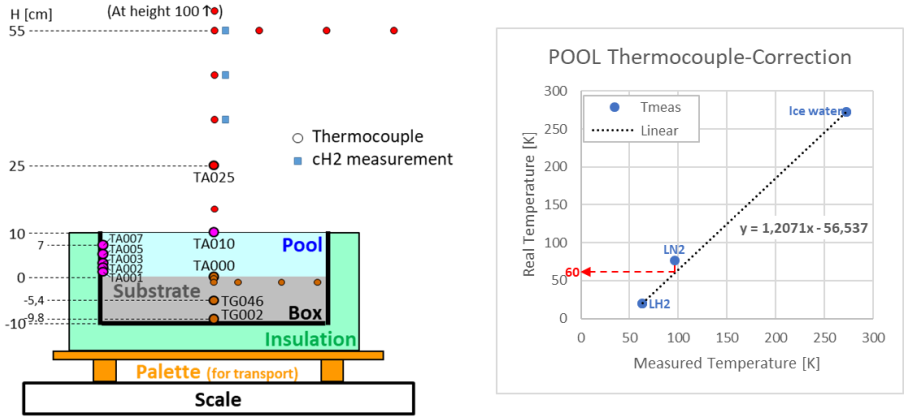

Figure 2. Sensor positions and determination of formula for temperature correction (right).

All thermocouples used in the experiments were of the same type (sheathed thermocouples type K, d = 1 mm) manufactured at KIT-workshop from the same batch. The thermocouples are not specified for the use in cryogenic conditions, so they were tested in ice water (T ≈ 273 K) and in boiling liquid nitrogen (LN2, T ≈ 80 K) prior to the experiments and in boiling LH2 (T ≈ 20 K) during the experiment itself. The right part of Fig. 2 shows that great deviation was found for the cryogenic temperatures. To facilitate the interpretation of the temperature readings, the temperature values were corrected after the tests using a linear fit through the values for ice water and LH2 (without taking into account the value for LN2) to achieve values close to 20 K for the temperature of LH2. Polynomial fits were neglected since they produced strange phenomena for temperatures above 0 °C. Unfortunately, the chosen correction leads to a significant mismatch for the temperature of LN2, since the corrected temperature yields 60 K (red arrow in graph). However, the main purpose of the thermocouple measurements inside the pool was not to determine precise temperature values below 100 K, but to identify the presence of LH2 by measuring a quasi-stationary temperature value significantly below the temperature of LN2.

The ambient wind conditions were recorded with an ultrasonic anemometer (Young, Model 81000) that is capable of recording the wind velocity in three dimensions. For safety reasons the device was positioned in a distance of approx. 15 m behind the wall with the BOS-background pattern, close to the tent, from where the POOL-facility was controlled.

The tent with the control computer of the facility was located in approx. 10 m distance behind the wall with the BOS-background pattern, but after the initiation of an experiment this computer was controlled remotely from a shelter in a distance of approx. 100 m to the facility. The control computer was also used to save all sensor records (temperatures, H2-concentrations, ambient wind conditions) with a measuring frequency of 10 Hz via LabView.

3.0 EXPERIMENTAL

For the LH2-pool generation a hand valve at the rear end of the trailer had to be opened manually (always to the same degree of valve opening), but due to safety reasons the closure of the release valve was done remotely using a safety mechanism of the trailer. A measurement of the LH2-flow velocity was not possible, since no such measurement is foreseen at the trailer and on the site, no suitable measuring device for cryogenic application was available.

In the experiments on LH2-pools the substrate filled box was usually filled three times to cover different degrees of pre-cooling of the substrate. Furthermore, it turned out that all sensor records showed less fluctuations when the pool was generated above a pre-cooled substrate. The data on temperature and H2-concentration distribution above the facility as well as the BOS-photos and movies were mainly used to determine promising ignition positions for the ignited POOL-experiments that will be published separately.

In four experiments “artificial wind” from a large fan was used to investigate the influence of side wind on the LH2-pool formation and evaporation. The fan was positioned in front of the protective wall of concrete blocks at the rear end of the trailer, to produce side wind of constant velocity and direction. In pre-experiments without substrate boxes, where the ultrasonic anemometer was positioned on the spot of the pool center, the rotation speed of the fan was adjusted to produce wind with a velocity of approx. 4 m/s in the measuring position. This rotation speed remained unchanged in all experiments with “artificial wind”.

Figure 3. Photo of an experiment without “artificial wind” (left), experimental setup with fan (center) and experiment with “artificial wind” (right).

3.1 Test Matrix

Table 1 shows the test-matrix for the 10 experiments on unignited LH2-spills that were performed with the POOL-facility and the four substrates available. Apart from the substrate, mainly the wind conditions were varied in the tests.

Table 1: Test matrix of the unignited POOL-experiments

Substrate	Fills	Wind	Comments
Concrete01	2	natural	no scales
Concrete02	4	natural	
Concrete03	3	artificial	
Sand01	3	natural	
Sand02	3	artificial	no wind data
Sand03	3	artificial	

Substrate	Fills	Wind	Comments
Gravel01	3	natural	
Gravel02	3	natural	Gas-Samples
Gravel03	3	artificial	Gas-Samples
Water01	3	natural	

3.2 Test Procedure and Facility Behavior

3.2.1 Pool Formation and Evaporation above Concrete or Sand as a Substrate

The test procedure and the typical behavior of an unignited POOL-experiment with concrete or sand as a substrate shall be explained based on experiment Sand02 with "artificial wind". Fig. 4 shows a summarizing graph with selected temperature signals and the LH2-mass for this experiment.

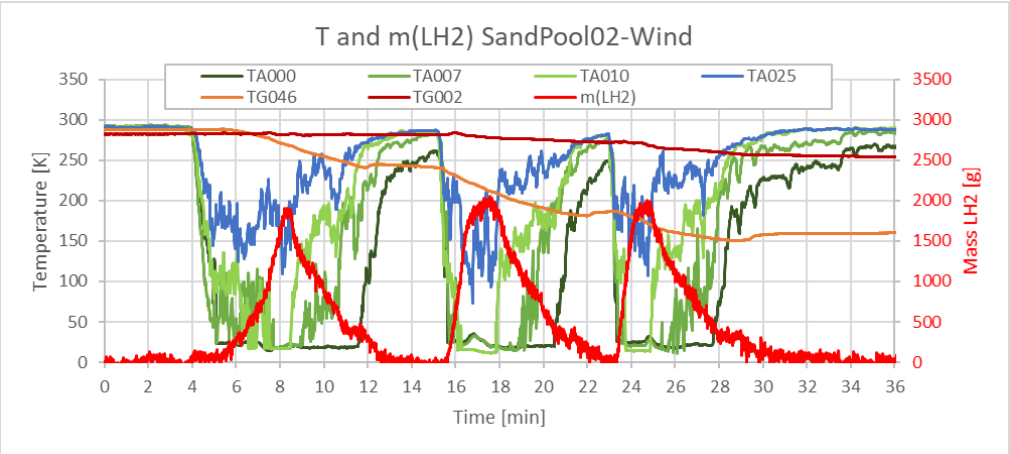

Figure 4. Summarizing graph of selected temperature signals and the LH2-mass for experiment Sand02 with "artificial wind".

In Fig. 4, the LH2-weight (red line, right ordinate) and selected temperatures inside the substrate (brown lines), inside the pool (green lines) and above the pool (blue line) are plotted. The fast temperature decreases in the positions above the substrate (green and blue lines) after t ≈ 4 min indicate that the LH2-release into the box was initiated at this point in time. In the initial phase of the release a flow of cold gaseous hydrogen (GH2) is directed into the box, since the super insulated hose has to be cooled down to approx. 20 K before LH2 actually reaches the substrate inside the box. In the experiments with the sand pool, a baffle plate is utilized to avoid the blow out of larger quantities of sand by this stream of cold gas, as it was observed in the first experiment with this substrate. When LH2 reaches the substrate, it immediately evaporates until the substrate surface is also cooled down to the boiling temperature of LH2. As soon as a LH2-pool starts to form above the substrate surface (t ≈ 5 min) the signal of TA000 (dark green curve in Fig. 4), measuring the temperature in the height of the substrate surface, remains stable at the temperature of boiling LH2 (approx. 20 K) and the weight signal starts to increase. During the following 3.5 minutes, the mass of LH2 in the pool increases constantly, as the increasing weight signal indicates. As soon as the thermocouples TA007 and TA010, in heights of 7 cm and 10 cm above the substrate surface, are also covered by the LH2-level (t ≈ 7.5 min), stable values close to 20 K are also measured by these sensors. Due to the vigorous boiling of the pool, all thermocouples inside the pool measure strong temperature fluctuations before they reach the steady state level. Similar fluctuations are also measured by the thermocouples above the pool, especially in the lower positions (e.g. TA025). The LH2-release is stopped approx. 40 s after the LH2 level has reached the upper rim of the box (TA010), at a weight of approx. 1900 g, as the beginning decrease of the weight signal and the fast temperature increase in a height of 25 cm above the substrate surface (TA025) indicate. The LH2-pool then evaporates continuously and passes the filling levels of 10 cm and 7 cm height at t ≈ 8.5 min and t ≈ 9 min (TA010 and TA007). At t ≈ 11.5 min, also the temperature at the substrate surface starts to increase and thus the complete LH2-pool above the upper substrate level has evaporated. The remaining mass of approx. 400 g might be due to LH2 still existing in gaps in between the steel box and surrounding insulation material, or in pits that were formed in the sand by the first flow of GH2 in the initial phase of the H2-release, or the remaining weight is due to condensed air components and humidity. When the weight of the pool has approached zero level, the box has warmed up to almost ambient temperature in most measuring positions above the substrate (t ≈ 15 min). During the first

filling, the temperature measured close to the ground level of the box (TG002) remains almost unchanged at 280 K, while in almost half the substrate height (TG046) it had decreased slowly from ambient level to 240 K.

Shortly after t ≈ 15 min the second filling is initiated, but this time the pre-cooled substrate allows a much faster filling of the box with LH2, as the fast temperature decays of the three pool-thermocouples (green curves in Fig. 4) indicate. The pool is filled to the upper rim (mLH2 ≈ 1900 g) and shows a slight overflow (t ≈ 17.5 min to 18 min, stagnating weight) before the LH2-release is stopped. Subsequently the LH2-pool evaporates to the same residual weight as after the first filling (mLH2 ≈ 400 g), when, at t ≈ 20.5 min, the temperature at the substrate surface starts to rise. During the second filling the temperature at half the substrate height further decreased to approx. 180 K, and also the temperature close to the ground level of the box shows a temperature decrease by approx. 10 K.

The third filling takes place from t ≈ 23 min to t ≈ 25 min, and shows a similar but faster course as observed for the second filling. When the LH2-release was stopped the pool-inventory had a mass of approx. 1970 g, and when the pool had evaporated (t ≈ 28 min, mLH2 ≈ 400 g), the facility was left to warm up to ambient temperature before the data acquisition was stopped. The minimum temperatures measured inside the substrate after the third filling were 150 K (TG046) and 255 K (TG002).

3.2.2 Pool Formation and Evaporation above Water as a Substrate

Only one experiment with water as substrate was performed. In principle the same behavior as for the pools above concrete and sand was observed, but the details of the experiment are very different. Therefore in Fig. 5 the summarizing plot of this experiment is depicted together with a photograph taken shortly after the experiment.

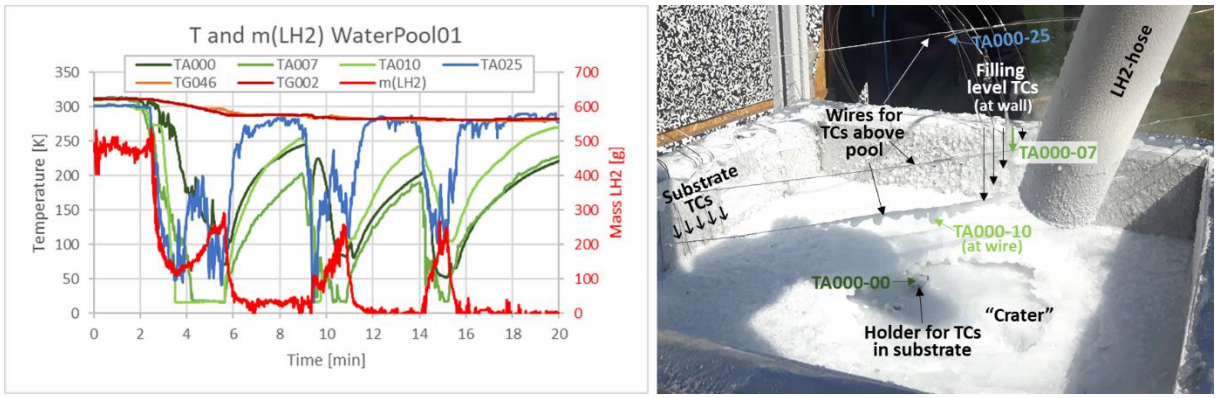

Figure 5. Summarizing graph of experiment Water01 (left) and photo of the facility after the test with sensor locations (right, TC = Thermocouple).

The summarizing plot shows that shortly after the beginning of the LH2-release (t ≈ 120 s), the mass of the facility strongly decreases by approx. 200 g before the actual LH2-pool formation starts to increase the weight (scales signal in Fig. 5 tared to final weight of pool). The strong mass decrease occurs due to water that is blown out of the pool due to rapid phase changes of the LH2 that is exposed to water at almost ambient temperature. As the photo in the right part of Fig. 5 demonstrates, a crater due to expelled water was still visible when the facility could be re-approached several minutes after the test. Together with the beginning of the pool formation inside the facility (t ≈ 210 s), the thermocouple at the upper rim of the pool (TA000-10) already detects the constant LH2-temperature, although the sensors below it (e.g. TA000-07 and especially TA000-00 at the substrate surface) do not yet detect such low temperatures. This strange behavior might be due to splashing water that freezes at the tip of the thermocouples as ice, which is then further cooled by splashes of LH2 or clouds of cold evaporated LH2. So the complete instrumentation of the pool was found to be "blind" in the test (except for the scales). The behavior did not improve in the subsequent fillings of the pool and thus the experiment was

aborted. So the pool was not filled completely with LH2 (weight increase by approx. 1700 g) in all three attempts, for safety reasons the filling was aborted at the much lower level of approx. 250 g.

3.2.3 Pool Formation and Evaporation above Gravel as a Substrate

Three unignited pool experiments with gravel as substrate were performed. Compared to the other experiments this substrate showed a significantly different behavior. The summarizing plot of experiment Gravel02 is depicted in Fig. 6.

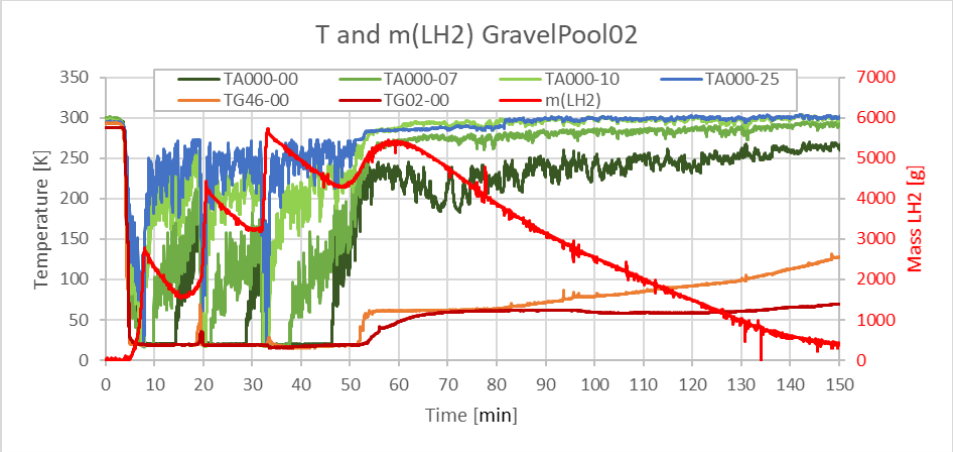

Figure 6. Summarizing graph of experiment Gravel02.

For the generation of the three LH2-pools above gravel as substrate much more time was needed than in the experiments with the other substrates. Since the LH2 flow rate was similar in all experiments, also much higher LH2-inventories were used in the experiments with gravel. The main reason for these differences is the high porosity of the substrate, which consists of massive, almost spherical stones that are loosely packed in the volume of the lower half of the box. Unlike the other substrates with much lower porosity, which slowly cooled from the surface into the bulk material by heat transfer, the gravel bed is massively penetrated by LH2 through the large gaps in between the stones. This results in a much larger surface for the heat transfer into the substrate and much more free volume that can be occupied by the LH2 pool.

Before an LH2 pool can be formed around a stone, at least its surface must have cooled down to 20 K. This means that cold stones at this temperature are exposed to the ambient air when the pool has completely evaporated. Since the temperature of the stones is then far below the boiling and melting temperatures of the main air components nitrogen and oxygen ($T_b(N_2) \approx 77$ K, $T_m(N_2) \approx 63$ K, $T_b(O_2) \approx 90$ K, $T_m(O_2) \approx 55$ K) massive condensation or desublimation of air components occurs. Most likely, this is the reason for the large steps in the weight records of all experiments with gravel, in which a massive increase of residual weight after each pool evaporation period is observed. The evaluation of these processes is much more complicated and therefore the experiments with gravel are not discussed further in this paper.

4.0 RESULTS AND DISCUSSION

4.1 Pool Evaporation above Concrete or Sand as a Substrate

For the evaluation of pool evaporation, mainly the weight signal and the signals of the seven thermocouples inside the pool (from substrate surface to upper rim of box) are used. The evaluation of the various experiments is explained based on experiment Concrete02, and so a summarizing graph of this experiment is shown in Fig. 7.

As explained above, the thermocouple records show a stable value close to 20 K as soon as they are covered by LH2, and a fast temperature increase to higher gas temperatures, when the LH2-level falls below their position. When these points in time are tracked down in the signal of TA007 (positioned 7 cm above the substrate surface), the times when the LH2-level passes a height of 7 cm during the evaporation process can be determined (dashed black vertical lines in Fig. 7). For the three points in time found in the above example, roughly the same mass of $m_{7cm} \approx 1240$ g in the pool is obtained (dashed horizontal black line). When the LH2-pool has completely evaporated (increase in signal of TA000 positioned at substrate surface), a remaining additional mass of $m_{Rem} = 300$ g due to LH2 in gaps or frozen ambient air components is still measured by the scale.

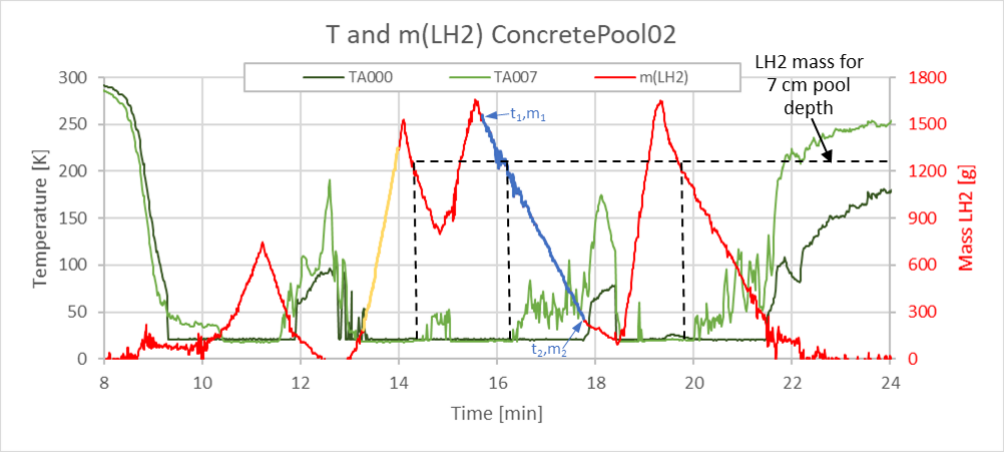

Figure 7. Summarizing graph of experiment Concrete02 (yellow and blue highlighted sections are examples for close-to-linear parts of the mass curve that are used for further evaluation).

With these readings, the actual mass of hydrogen in the pool at the point in time when the filling level decreases below 7 cm can be calculated as follows

$$m_{LH2@7cm} = m_{7cm} - m_{Rem} = 0.940 \text{ kg}, \quad (1)$$

where $m_{LH2@7cm}$ - mass of hydrogen in the pool at filling level 7 cm, kg; m_{7cm} – measured mass for pool height of 7 cm, kg; m_{Rem} – remaining additional mass after evaporation, kg.

A pool with a height of 7 cm above a square base area with a side length of 50 cm has a volume of

$$V_{Pool@7cm} = L^2 \cdot h = 0.0175 \text{ m}^3, \quad (2)$$

where $V_{Pool@7cm}$ – pool volume for 7 cm height, m³; L – side length of square pool ground face, m; h – height of pool, m.

This results in a density for the LH2 in the pool of

$$\rho_{LH2pool} = m_{LH2@7cm} / V_{Pool@7cm} = 53.7 \text{ kg/m}^3, \quad (3)$$

where $\rho_{LH2pool}$ – density of LH2 in the pool, kg/m³; $m_{LH2@7cm}$ – LH2 mass in pool of 7 cm height, kg; $V_{Pool@7cm}$ – volume of pool of 7 cm height, m³.

which is low compared to a value of $\rho_{LH2} \approx 70.8$ kg/m³ found for the density of LH2 in literature. This indicates that the pool contains an amount of approx. 76% LH2 and 24% void. A rather high void fraction in the pool can be expected after the cool-down phase with a very high initial superheat of close to 260 K and vigorous boiling.

The left part of Fig. 8 shows details of the signals of the pool-thermocouples for the second filling and the third evaporation period of the experiment, as indicated by the highlighted yellow and blue sections in the weight curve of Fig. 7. The rather short evaporation and refilling periods in between t = 845 s and t = 910 s are omitted for clarity. For the second filling period (t ≈ 755 to 845 s, yellow arrows in left part of Fig. 6), no clear order of thermocouples reaching LH2-temperature in positions below 7 cm above the substrate surface can be determined, since the pool is vigorously boiling despite the pre-cooling during the first (incomplete) filling. Due to the boiling, the thermocouples are repeatedly exposed to droplets of LH2, although the filling level has not yet reached their positions. So the thermocouples' signal cannot be used for a detailed analysis of the pool formation.

In contrast to this, after the third filling period (t ≈ 890 to 935 s) the pool is completely filled to a height of 10 cm with LH2, before it starts to vaporize. Then, as soon as the LH2 level passes a thermocouple position, the temperature jumps to a higher gas temperature, as highlighted by the blue arrows in the left part of Fig. 8. So, for the evaporating pool, passing-times of the LH2-level for the seven pool-thermocouples from 10 to 0 cm height above the substrate surface can be clearly identified.

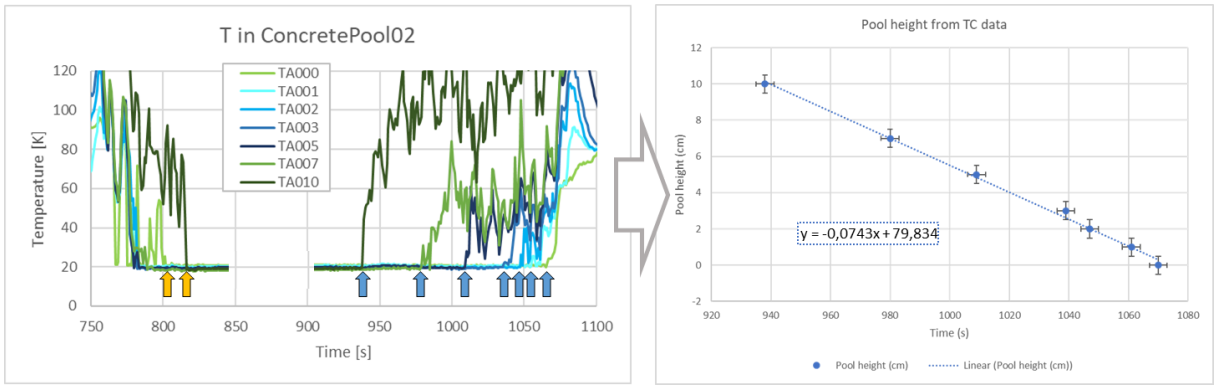

Figure 8. Determination of LH2-pool formation and evaporation rate based on TC-signals (short evaporation and refilling periods from t = 840 s to 910 s omitted in left graph for clarity).

When these pool heights are plotted over time, a vaporization velocity of the boiling LH2 pool in the form of a height reduction velocity $(dh/dt)_{boil}$ = 0.0743 cm/s can be determined from the slope of the curve (Fig. 8, right).

For the blue highlighted part of the weight-curve in Fig. 7, a weight loss velocity can be determined, using the values for the beginning (index 1) and end (index 2) of the blue line:

$$dm_{H2}/dt = (m_1 - m_2)/(t_2 - t_1) = 0.0105 \text{ kg/s}, \quad (4)$$

where dm_{H2}/dt – weight loss velocity, kg/s; m_1, m_2 – weight of pool at beginning/end of time span under consideration, kg; t_1, t_2 – beginning/end of time span under consideration, s.

For an estimation of the density of the boiling pool the following relation is used:

$$dm_{H2}/dt = \rho_{boil} \cdot L^2 \cdot (dh/dt)_{boil}, \quad (5)$$

where dm_{H2}/dt – measured weight loss rate of the pool from Eq. (4), kg/s; L – side length of the square pool ground face, m; $(dh/dt)_{boil}$ – recession velocity of pool surface determined graphically in the right graph of Fig. 8; m/s, ρ_{boil} – density of the boiling pool, kg/m³.

When Eq. (5) is solved for the density of the boiling pool, a value of ρ_{boil} = 56.5 kg/m³ is obtained, which corresponds to 80% of the LH2 density at 1 bar pressure (70.8 kg/m³) and a GH2 void fraction of 20%, which is close to the estimated value of 24% void determined above.

The heat flow from the concrete into the LH2 pool was estimated as

$$Q_{pool} = (dm_{H2}/dt) \cdot \Delta h_{fg} = 4725 \text{ W} \quad (6)$$

where Q_{pool} – heat flow from concrete into LH2 pool, W; dm_{H2}/dt – measured weight loss rate of pool from Eq. (4), kg/s; Δh_{fg} – heat of LH2 vaporization (450 kJ/kg [8]), J/kg.

The evaporation rate (dm_{H2}/dt) and the corresponding heat flow from the concrete into the LH2 pool decreased with increasing time due to the decreasing temperature gradient in the concrete. The measured heat flux density from the concrete into the LH2 can be expressed as follows:

$$q_{pool} = Q_{pool} / L^2, \quad (7)$$

where q_{pool} – heat flux density from concrete into LH2, W/m²; Q_{pool} – heat flow from concrete into LH2, W; L – side length of the square pool ground face, m,

With the area of the concrete surface being $L^2 = 0.25$ m², in the above example the measured heat flux density from the concrete into the LH2 is $q_{pool} = 18.7$ kW/m². Compared to this value, the heat flux to the pool from solar radiation is negligible, since, with the solar constant (1361 W/m²), a partial reflection of 25% on a clear day, and the solar inclination angle α for the time and location of the test (March, 49° northern latitude, α = 45°) q_{solar} is approx. 0.72 kW/m².

The evaporation of cryogenic fluids is governed by the heat conduction from the ground into the liquid pool. The phenomena might be described by a one-dimensional heat conduction equation, whose solution gives the LH2 evaporation rate in kg/s:

$$dm_{LH2}/dt = L^2 k \Delta T / [\Delta h_{fg} (\pi \alpha t)^{1/2}], \quad (8)$$

where L – side length of the square pool ground face, m; k – thermal conductivity of substrate, W/mK; ΔT – temperature difference between boiling temperature of liquid and environment, K; Δh_{fg} – heat of LH2 vaporization, J/g; α –thermal diffusivity of substrate, m²/s; and t – time for coverage of ground with liquid pool.

In the same way, the evaporation behavior for the remaining evaporation phases in experiment Concrete02 (except for the short phase 2, where only a section in the upper part of the pool evaporated) and all other experiments with concrete (except Concrete01, no weight data available) and with sand as substrate was investigated. The main results are summarized in Fig. 9, where experimental and calculated evaporation rates, the calculated density for LH2 in the boiling pool (ρ_{boil}) and the heat flux density from the substrate into the LH2 (q_{pool}) are plotted as a bar chart. Eq. (8) for the calculation of the evaporation rates was only applied to the first experiment of a series, since all following fillings started at a pre-cooled surface with a temperature far below ambient temperature, where also the temperature measurements of the thermocouples become inaccurate (see Fig. 2). Thus the temperature difference ΔT in Eq. (8) cannot be determined accurately for these phases.

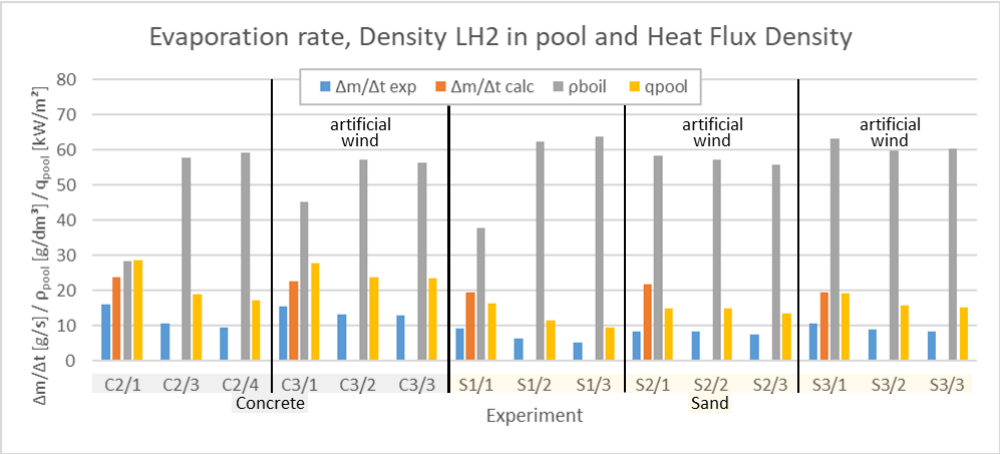

Figure 9. Experimental and calculated evaporation rate, density of LH2 in boiling pool (ρ_{boil}) and heat flux density from substrate into LH2 (q_{pool}) for experiments with the substrates concrete and sand.

A comparison of experimental and calculated evaporation rates shows reasonably good agreement, with at least similar values of the same order of magnitude. Problems may originate from the values for the thermal properties of the substrates (k and α in Eq. (8)), which were not measured for the substrates used, but taken from a general table in the internet [9]. Further uncertainties are connected with the beginning of the time interval t and the initial temperature for the determination of ΔT in Eq. (8), since the LH2 release always followed an exposure of the substrate to cold GH2, which was very long, especially for the first experiment of a series.

The measured evaporation rates show a similar behavior in all experiments performed. In general, the values determined for concrete were higher than for sand. During the first evaporation phase always the highest evaporation rate of an experiment is determined, since the substrate initially has ambient temperature. In the subsequent fillings, the pool is generated above a pre-cooled substrate, and so the driving force for the evaporation, the temperature difference between liquid and substrate, is smaller. In case of strong "artificial" side wind, the differences between the first and the subsequent evaporation rates become smaller, most likely due to the longer duration of the first filling procedure, that allows a more effective cooling of the substrate prior to the first evaporation phase.

Due to the most vigorous boiling in the first evaporation phase, the density of an evaporating pool is found to be lowest in the first evaporation phase of an experiment, where also the highest void fraction is to be expected. In the following evaporation phases, a less vigorous boiling above the pre-cooled substrate is observed and thus the density increases. In experiments with "artificial" side wind the density differences in between first and subsequent evaporation phases become much smaller, which is most likely due to the longer first filling phase and the resulting more effective cooling of the substrate prior to the first evaporation phase.

According to Eq. (6) and Eq. (7) the heat flux density is proportional to the measured evaporation rate and thus the behavior of the determined values for q_{Pool} is similar.

5.0 SUMMARY

In the POOL-facility at KIT a series of ten experiments on LH2 pool formation and evaporation was performed with the four different substrates concrete, sand, water and gravel. The facility mainly consists of an insulated box (L x W x H: 0.5 x 0.5 x 0.2 m³) that is filled up to half the height with the respective substrate. In four of the ten experiments, "artificial" side wind of known direction and velocity was applied using a large fan. In most of the experiments three fillings of the free volume in the box with LH2 were performed.

For reasons of space, the current article concentrates on the evaporation phases of the experiments, where evaporation rates were determined for 15 evaporation phases of five experiments with the two substrates concrete and sand. The single experiment with water as substrate and the first experiment with concrete were omitted due to incomplete data records, while the experiments with gravel were omitted due to complicated underlying processes in connection with frozen air compounds inside the LH2 pool.

Using the scale and thermocouple records, the evaporation rates above the substrates concrete and sand were determined for initial ambient and subsequent pre-cooled conditions of the substrate. The values determined during the evaluation showed good consistency.

Finally, an equation for the estimation of the evaporation rate of LH2 over non-porous solid surfaces was proposed that yielded reasonably good agreement with the experimental values. The experimental data follow the $t^{-1/2}$ dependence of the model quite well and heat transfer from the solid ground determines LH2 evaporation rates.

ACKNOWLEDGEMENTS

This research has received funding from the Fuel Cells and Hydrogen 2 Joint Undertaking under grant agreement No.779613 (PRESLHY), This Joint Undertaking receives support from the European Union's Horizon 2020 research and innovation programme, Hydrogen Europe and Hydrogen Europe research.

REFERENCES

1. Verfonderna, K., Dienhart, B., Pool spreading and vaporization of liquid hydrogen, *International Journal of Hydrogen Energy*, **32**, 2007, pp. 2106 – 2117.
2. Venetsanos, A.G., Bartzis, J.G., CFD Modelling of Large-Scale LH_2 Spills in Open Environment, |*International Journal of Hydrogen Energy*, **32**, 2007, pp. 2171 – 2177.
3. Venetsanos, A.G., Papanikolaou, E., Bartzis, J.G., The ADREA-HF Code for Consequence Assessment of Hydrogen Applications, *Journal Hydrogen Energy*, **35**, 2010, pp. 3908 – 3918.
4. Middha, P., Ichard, M., Arntzen, B.J., Validation of CFD Modelling of LH_2 Spread and Evaporation against Large-Scale Spill Experiments, *Journal of Hydrogen Energy*, **36**, 2011, pp. 2620 – 2627.
5. Brambilla, S., Manca, Accidents Involving Liquids: A Step Ahead in Modelling Pool Spreading, Evaporation and Burning, *Journal of Hazardous Materials*, **161**, 2009, pp. 1265 – 1280.
6. Shirai, Y., Tatsumoto, H., Shiotsu, M., Hata, K., Kobayashi, H., Naruo, Y., Inatani, Y., Boiling Heat Transfer from a Horizontal Flat Plate in a Pool of Liquid Hydrogen, *Cryogenics Journal*, **50**, 2010, pp. 410 – 416.
7. Dienhart B., Ausbreitung und Verdampfung von fluessigem Wasserstoff auf Wasser und festem Untergrund, *Research Center Juelich Report*, No. Juel-3155, 1995.
8. Zhang, Y., Evans, J.R.G. and Yang, S., Corrected Values for Boiling Points and Enthalpies of Vaporization of Elements in Handbooks, *J. Chem. Eng. Data*, **56**, 2011, pp. 328–337.
9. German Wikipedia (March 30 2023) *Temperaturleitfähigkeit*, https://de.wikipedia.org/wiki/Temperaturleitf%C3%A4higkeit